ISSN 2394-3777 (Print)
ISSN 2394-3785 (Online)
Available online at www.ijartet.com

International Journal of Advanced Research Trends in Engineering and Technology (IJARTET)
Vol. 5, Issue 4, April 2018

Anomaly Detection in Hyper Spectral Images

D. RamKumar [#1], R. Sahila [#2], R. Muthu selvi[#3].
#1 Associate professor (Department of ECE), Bharath Niketan Engineering College.
#2 Assistant professor (Department of ECE), Bharath Niketan Engineering College.
#3 PG Scholar (Department of ECE), Bharath Niketan Engineering College.

Abstract: Hyper spectral remote detecting symbolism contains significantly more data in the ghastly area than does multi spectral symbolism. The sequential and bounteous phantom signs give an awesome potential to characterization and irregularity location. A data set will be considered with Peculiarity spots. Utilized systems to enhance the estimation of foundation data both the foundation and irregularity data are removed and after that the recognition will be finished. And furthermore recognize peculiarities from hyper phantom picture. To gauges both foundation data and inconsistency data and after that uses the data to lead abnormality location.

Keywords: HSI, RSAD, Anomaly, MATLAB.

I. INTRODUCTION

Anomaly detection is an intriguing issue in hyper unearthly picture preparing and furthermore no objective or foundation ghostly data is accessible during the time spent location, oddities still have two attributes that make them exceptions: their other worldly marks are not quite the same as the encompassing pixels oddities happen in a picture with low probabilities. As indicated by the two attributes, factual models have been created to figure the likelihood of being an inconsistency for a pixel under test (PUT). The principle supposition is that its experience takes after a multivariate ordinary dissemination. As indicated by this suspicion, the Reed– Xiaoli locator (RXD) was created and has been extensively utilized for anomaly detection. It applies the likelihood thickness capacity of a multivariate typical circulation figuring the likelihood of a PUT being a piece of the foundation. Notwithstanding, the supposition, held by the RXD, that the foundation is a multivariate typical circulation is excessively basic for some genuine situations. This is on account of, more often than not, a scene contains an assortment of articles that are too frightfully complex to be considered as a multivariate typical dissemination. Along these lines, this supposition may prompt an expansion of the false caution rate (FAR) of the RXD.A assortment of methodologies have been actualized to stifle the FAR of the RXD. A few strategies center around how to make the foundation more like a multivariate typical appropriation. They refine the foundation by expelling peculiarities or decreasing the heaviness of the inconsistencies out of sight samples. These calculations incorporate the blocked versatile computationally proficient exception nominator (BACON), the arbitrary determination based irregularity indicator (RSAD), the weighted-RXD (W-RXD), and the probabilistic abnormality finder (PAD). Both BACON and RSAD mean to keep defilement from bizarre marks while assessing foundation data. The W-RXD can decrease the heaviness of odd pixels or commotion flags and increment the heaviness of the foundation tests while evaluating foundation measurable data. All are capable in spotting oddities as exceptions. In any case, it is discernible that these enhanced techniques just gauge data of the foundation, with the exception of the PAD. The PAD calculation is an unsupervised probabilistic abnormality indicator in view of evaluating the contrast between probabilities of irregularities and their background. It gauges the data of both the foundation and the oddity for the inconsistency identification process. In this paper, a review of the six oddity finders, i.e., the great RXD calculation (GRXD and LRXD), the BACON, RSAD, W-RXD, and PAD, is given. Also, utilizing genuine hyper unearthly informational indexes, two investigations were led to test and assess the exhibitions of the six detectors. The capacity of recognition and the time utilization of these calculations are talked about utilizing the hyper ghostly informational collections.

II. MULTIVARIATE NORMAL DISTRIBUTION MODEL FOR ANOMALY DETECTION

2.1 RXD

The RXD accept that the foundation in a hyper spectral picture takes after a multivariate typical dissemination, which can be depicted as follows. Let H1 be the objective flag and H0 be the foundation flag. Accordingly, the location issue can be characterized as H0 : x = b ,H1 : x = s + b where x is an example pixel vector; s is the objective flag; and b is the foundation flag that is accepted as a multivariate typical dissemination. Mean

ISSN 2394-3777 (Print)
ISSN 2394-3785 (Online)
Available online at www.ijartet.com

International Journal of Advanced Research Trends in Engineering and Technology (IJARTET)
Vol. 5, Issue 4, April 2018

vector μ and co-difference network S of the foundation are displayed as a various typical conveyance N(μ, S). Thusly, x|H0 are demonstrated as N(μ, S), and x|H1 are displayed as N(μ+ s, S). In view of measurement learning, we can acquire the accompanying likelihood/where K is the quantity of groups in a hyper ghostly image. Since a peculiarity xs is relied upon to be essentially not quite the same as the foundation in ghastly space, p(xs|H0) ought to be little for an irregular pixel. In this manner, for a given foundation, as is settled, (xs - μ)TS-1(xs - μ) ought to be bigger for an abnormal pixel than for a foundation pixel. In view of this perception, RXD utilizes the accompanying articulation to identify anomalies: $RXD(\mathbf{x}) = (\mathbf{x} - \mu)^T\mathbf{\Sigma}^{-1}(\mathbf{x} - \mu)$.t is noticeable that there are several ways to obtain samples for estimating **Σ** and μ of the background. The global-RXD (GRXD) and local-RXD (LRXD) are two common methods using different strategies. The GRXD is given by $DGRXD(\mathbf{x}) = (\mathbf{x} - \mu G)$ $T\mathbf{\Sigma}G-1(\mathbf{x} - \mu G)$ where μ_G and $\mathbf{\Sigma}_G$ are the mean vector and covariance matrix of all pixels in the image. Not the same as the GRXD, the LRXD utilizes μ8, the mean estimation of its eight encompassing pixels. At that point, it is given by DLRXD(x) = (x - μ8) TSG-1(x - μ8). The LRXD for the most part utilizes SG as the co-change network rather than S8. The reason is, in hyper ghostly information, the quantity of ghastly groups is considerably higher than 8; therefore, S8 is a solitary network with no reversal.

2.2 BACON

The BACON is a calculation to spot anomalies in multivariate and relapse information. It utilizes two techniques to actualize the identification (1) thresholding RXD estimations of pixels to refine the foundation and (2) diminishing the quantity of foundation tests to build the time productivity. The BACON calculation incorporates the accompanying advances:

Step 1. Register the RXD score for each PUT. Select m= cK pixels with little RXD scores as the underlying foundation subset, where K is the quantity of groups, c is a little whole number picked by the information examiner, and c ought to be more noteworthy than 1 so the state of m >K can be met.

Step 2. Acquire the square base of the RXD scores in light of the present foundation subset.

Step 3. Select those pixels whose square root estimations of RXD scores are littler than cnKr?K,a as new foundation tests, where ?K,a is the square base of the 1 - a percentile of the chi-square dissemination with K degrees of opportunity, and cnKr is figured as cnKr = cnK + chr,where n is the aggregate number of pixels, and r is the quantity of pixels in the present foundation subset.

Step 4. Emphasize Steps 2 and 3 until the measure of the foundation subset never again changes.

Step 5. Guide anomalies to the picture space.

2.3 W-RXD

So as to decrease the sullying of atypical pixels and enhance the estimation of the co-difference framework for the foundation data, the W-RXD allocates diverse weights to the foundation tests. In the regular RXD, when we ascertain S and μ, the heaviness of every pixel is the same, i.e.N1, where N is the quantity of thought about examples. Keeping in mind the end goal to hold the foundation flag and lessen the non-foundation flag, the W-RXD doles out those pixels that are close to the background a higher weight than the weight assigned to the pixels that are far away from the background.

III. Experiments with Hyperspectral Image Data

In this section, two hyperspectral images are used for an experimental evaluation of the six detectors discussed above. In the following, we describe the data sets and analyze the results produced by the different anomaly detectors.

3.1 The World Trade Center (WTC)

The first hyperspectral data set was collected by the Airborne Visible Infra-Red Imaging Spectrometer (AVIRIS) over the WTC area in New York on 16 September 2001 (just five days after the terrorist attacks that collapsed the two main towers in the WTC complex). A segment of 200 × 200 pixels (with 224 phantom groups covering an otherworldly range in the vicinity of 0.4 and 2.5 μm) was chosen for the test in this investigation. The informational index secured the problem areas relating to dormant flames at the WTC, which can be considered as peculiarities. false shading composite picture of the bit of the AVIRIS picture chose for the test, shows a ground-truth information picture, which demonstrates spatial areas of the problem areas gave by the United States Geological Survey (USGS). The ground truth Image was used to evaluate the performances of the different anomaly detectors.

ISSN 2394-3777 (Print)
ISSN 2394-3785 (Online)
Available online at www.ijartet.com

International Journal of Advanced Research Trends in Engineering and Technology (IJARTET)
Vol. 5, Issue 4, April 2018

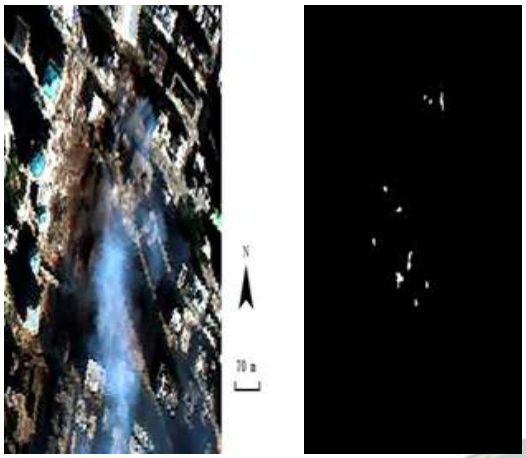

(a) (b)

Figure 3.1.(a)AVIRIS picture covering the World Trade Center (WTC) in New York City; (b) ground-truth outline spatial areas of problem area fires, accessible from the United States Geological Survey.

This examination executed the GRXD, LRXD, BACON, RSAD, W-RXD, and PAD and thought about their outcomes. There were no less than two criteria that were utilized to assess the exhibitions of the identification calculations: beneficiary working trademark (ROC) bends and the territory under the ROC bends (AUC). The x-hub of the ROC is the false caution rate (FAR), and the y-hub of ROC speaks to the likelihood of recognition. Accordingly, it builds up a correspondence between the location likelihood and the FAR. The upper and left bends demonstrate better discovery exhibitions. The dark scale pictures made utilizing these indicators are appeared in Figure 3. The measurement and extending data for the six dim scale pictures is abridged in Table 1. We could recognize some fire spots by their high brilliance esteem. The ROCs of the talked about techniques are introduced in Figure 4, AUCs are appeared in the BACON and the RSAD shared the most noteworthy AUC esteem among the majority of the calculations.

However, the BACON took the longest time (97.03 s) among the six detectors, and the RSAD took some time, too (49.55 s). The main reason for this is that both the BACON and the RSAD are iterative algorithms, with great capabilities to purify the background albeit consuming much computation time. According to the AUC values and time consumption, the GRXD was better than the LRXD. The PAD outperformed the W-RXD with a larger AUC value, but the processing time was longer (20.91 s). The PAD and the W-RXD possess advantages when an image is large, as they keep the best balance on time consumption and detection performance among these detectors.

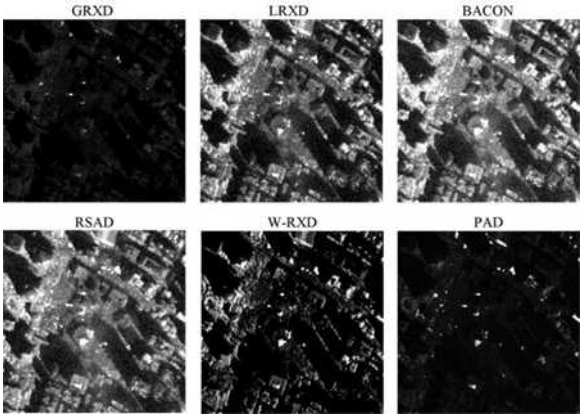

Figure 3. Detection results created by different algorithms with the WTC data.

IV. PROPOSED SYSTEM

4.1 RSAD

Different from the BACON, the RSAD algorithm randomly selects representative background samples from the image to estimate background statistical information, identifies anomalies via statistical differences, and finally fuses all detection results. The steps of the RSAD are described as follows:

Step 1. Randomly select background pixels as the initial background subset of observed pixels from a hyperspectral image.

Step 2. Compute the square root of the RXD value of each pixel vector based on the current background subset.

Step 3. Select those pixels whose square root values of RXD scores are smaller than $c_{nKr}\chi_{K,\alpha}$ as the new background samples pixels. The procedures to compute c_{nKr} are the same as those for the BACON.

Step 4. Iterate Steps 2 and 3 until the size of the background subset no longer changes.

Step 5. Label the pixels excluded by the final background subset as anomalies.

4.2 SpecTIR Data

The second data set was collected in the SpecTIR Hyperspectral Airborne Rochester Experiment (SHARE). The data set was collected on 29 July 2010 by the ProSpecTIR-VS2 sensor containing 360 bands from 390–2450 nm with a 5 nm spectral resolution. The ground resolution is approximately 1 m. In the image, road and vegetation are the main backgrounds, and red and blue fabrics (sized 9, 4 and 0.25 m^2 respectively) were placed purposely as anomalies. We selected an area of 180 × 180 pixels that contains these anomalies, as displayed in Figure 3.2(a), for the experiment. Figure 3.2(b) displays

ISSN 2394-3777 (Print)
ISSN 2394-3785 (Online)
Available online at www.ijartet.com

International Journal of Advanced Research Trends in Engineering and Technology (IJARTET)
Vol. 5, Issue 4, April 2018

the ground-truth location of the anomalies in the experiment.

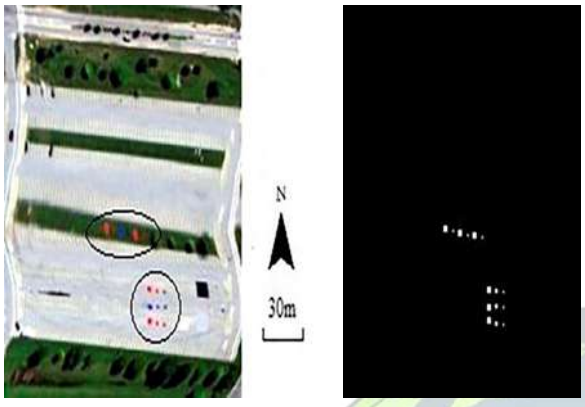

Figure 3.2. (a) The SpecTIR hyperspectral image. The anomalies were highlighted by black ellipses; (b) Ground-truth information of the anomalies.

The location comes about got from the SpecTIR picture are introduced. The twofold pictures acquired in the wake of thresholding the identification. The measurement and extending data for the six grayscale pictures is outlined. From the parallel pictures, it is observable that the BACON, RSAD, W-RXD, and PAD could identify a bigger number of little irregularities than the RXD and the LRXD. All the more particularly, the BACON, RSAD, W-RXD, and PAD could distinguish five sub-pixel boards (0.25 m2) out of six, while the GRXD and LRXD could not recognize any of them. The ROC bends for the SpecTIR information are in the AUC and the handling time of the six algorithms. The computational many-sided quality of every one of the six locators is O(N · K2), where N is the quantity of pixels, and K is the quantity of bands. The exhibitions of the BACON, RSAD, W-RXD,and PAD were nearly the same for this informational index. The four calculations were superior to the GRXD and the LRXD, which was demonstrated by the ROC bends and the AUC esteems. BACON, RSAD, W-RXD,and PAD outperformed the GRXD and the LRXD in detecting sub-pixel anomalies. The AUC of GRXD was slightly larger than the AUC of the LRXD, and the GRXD also cost less time than the local algorithm.

The BACON, RSAD, W-RXD, and PAD outflanked the GRXD and the LRXD in distinguishing sub-pixel peculiarities. The AUC of GRXD was somewhat bigger than the AUC of the LRXD, and the GRXD additionally cost less time than the neighborhood calculation. The BACON and the RSAD took additional time than the W-RXD and the PAD in light of the fact that the BACON and the RSAD are iterative calculations and lead the discovery procedure a few times previously end. The PAD and W-RXD just play out the discovery procedure twice as the primary recognition process plans to arrange oddities from the picture (the PAD) or acquire weights for the pixels (the W-RXD). Therefore, the PAD and the W-RXD can identify the majority of the irregularities and keep up the time-productivity for the SpecTIR information.

V. Result And Discussion

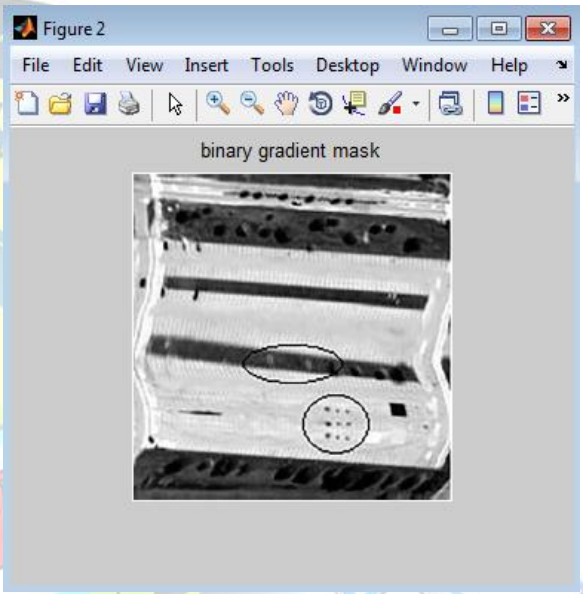

Figure 5. Binary gradient Mask image

The binary gradient mask image which is the interim file generated while detecting the anomalies. This picture is caught from the MATLAB instrument while execution of the venture.

ISSN 2394-3777 (Print)
ISSN 2394-3785 (Online)
Available online at www.ijartet.com

International Journal of Advanced Research Trends in Engineering and Technology (IJARTET)
Vol. 5, Issue 4, April 2018

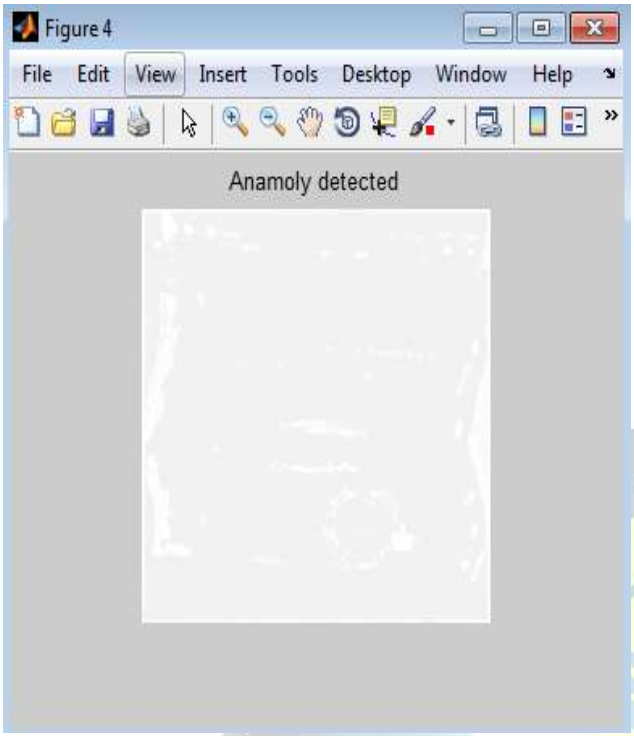

Figure 5.1 Anomaly detected Image

Anomaly recognized Image inconsistency distinguished picture which obviously demonstrates the shrouded oddities as of now existed in the dataset. The peculiarities were available around the sides of the pictures. Also the pre-known anomalies were also marked.

VI. CONCLUSION

In this paper, another hyper spectral AD technique, called LLTSA-SSBJSR, is proposed. LLTSA-SSBJSR considers the spectral and spatial qualities and joins the spectral BJSR with the spatial BJSR to enhance the identification execution. The proposed algorithm was tested on synthetic and real hyperspectral data. The extensive experimental results show that LLTSA-SSBJSR generally achieves better detection performance than the PCA-LRX, PCA-LSD, SDI-LLE and BJSR algorithms. Parameter selection is also discussed in this paper. LLTSA-SSBJSR still has room for improvement. The parameter selection is mainly determined by experience and repeated experiments, and our future research will focus on how to quickly and effectively determine the optimal parameters.

REFERENCES

[1]. Banerjee, A.; Burlina, P.; Diehl, C. A support vector method for anomaly detection in hyperspectral imagery. IEEE Trans. Geosci. Remote Sens. 2006, 44, 2282–2291. [CrossRef]

[2]. Billor, N.; Hadi, A.S.; Velleman, P.F. BACON: Blocked adaptive computationally efficient outlier nominators. Comput. Stat. Data Anal. 2000, 34, 279–298. [CrossRef]

[3]. 3.Du, B.; Zhang, L. Random-selection-based anomaly detector for hyperspectral imagery. IEEE Trans. Geosci. Remote Sens. 2011, 49, 1578–1589. [CrossRef]

[4]. Gao, L.; Guo, Q.; Plaza, A.; Li, J.; Zhang, B. Probabilistic anomaly detector for remotely sensed hyperspectral data. J. Appl. Remote Sens. 2014, 8, 083538. [CrossRef]

[5]. Gorelnik, N.; Yehudai, H.; Rotman, S.R. Anomaly detection in non-stationary backgrounds. In Proceedings of the 2010 2nd Workshop on Hyperspectral Image and Signal Processing: Evolution in Remote Sensing, Reykjavìk, Iceland, 14–16 June 2010.

[6]. Guo, Q.; Zhang, B.; Ran, Q.; Gao, L.; Li, J.; Plaza, A. Weighted-RXD and Linear Filter-Based RXD: Improving Background Statistics Estimation for Anomaly Detection in Hyperspectral Imagery. IEEE J. Sel. Top. Appl. Earth Obs

[7]. Khazai, S.; Homayouni, S.; Safari, A.; Mojaradi, B. Anomaly detection in hyperspectral images based on an adaptive support vector method. IEEE Geosci. Remote Sens. Lett. 2011, 8 licensee MDPI, Basel, Switzerland. This article is an open access article distributed under the terms and conditions of the Creative Commons Attribution

[8]. Kwon, H.; Der, S.Z.; Nasrabadi, N.M. Adaptive anomaly detection using subspace separation for hyperspectral imagery. Opt. Eng. 2003, 42, 3342–3351. [CrossRef]

[9]. Kwon, H.; Nasrabadi, N.M. Kernel RX-algorithm: A nonlinear anomaly detector for hyperspectral imagery. IEEE Trans. Geosci. Remote Sens. 2005, 43, 388–397. [CrossRef].

[10]. Reed, I.S.; Yu, X. Adaptive multiple-band CFAR detection of an optical pattern with unknown spectral distribution. IEEE Trans. Acoust. Speech Signal Process. 1990, 38, 1760–1770. [CrossRef]

BIOGRAPHY

Dr. D. Ramkumar did his bachelor of engineering in Electronics and Communication Engineering from the Indian Engineering College and the Master degree in Applied Electronics with first class with distinction from Anna University. He received his Ph.D. (Image Processing) from Anna University. Currently he is working as a Associate professor in the department of ECE, Bharath Niketan Engineering College. His area of interest is image processing, biomedical, network and communication.

ISSN 2394-3777 (Print)
ISSN 2394-3785 (Online)
Available online at www.ijartet.com

International Journal of Advanced Research Trends in Engineering and Technology (IJARTET)
Vol. 5, Issue 4, April 2018

R. Sahila did her bachelor of engineering in Electronics and Communication Engineering from Arulmigu kalasalingam college of Engineering under Madurai Kamaraj University. And has a Master degree in Embedded System Technologies from Raja College of Engineering and technology under Anna University. Currently she is working as a assistant professor in the department of ECE, Bharath Niketan Engineering College. Her area of interest is Signal Processing, Embedded systems.

R. Muthu Selvi did her bachelor of Engineering in Electronics and Communication Engineering from Jansons Institute of technology under Anna University. And has a master degree in Communication systems from Bharath Niketan Engineering College under Anna University. Her area of interest is Image Processing, Computer Networks, and Digital Communication systems.